Topochemical bias in the hydrogen-bonded networks of guanidinium carboxybenzenesulfonates†

Veneta Videnova-Adrabińska,*[a] Ilona Turowska-Tyrk,[b] Teresa Borowiak[c] and Grzegorz Dutkiewicz[c]

[a] *Institute of Inorganic Chemistry and Metallurgy of Rare Elements, Wrocław University of Technology, 23 Smoluchowskiego St., 50-372 Wrocław, Poland. E-mail: veneta@ichn.ch.pwr.wroc.pl; Fax: +48 71 328 4330*
[b] *Institute of Physical and Theoretical Chemistry, Wrocław University of Technology, 27 Wybrzeża Wyspiańskiego St., 50-372 Wrocław, Poland*
[c] *Faculty of Chemistry, Adam Mickiewicz University, 6 Grunwaldzka St., 60-780, Poznań, Poland*

Received* (*in Montpellier*, *France*) *15th November 2000, Accepted 29th June 2001
First published as an Advance Article on the web 17th October 2001

Herein we describe the changes in the packing patterns and discuss the structural modifications in guanidinium carboxybenzenesulfonates G · CBS $[C(NH_2)_3]^+[XC_6H_4SO_3]^-$ (where X is the carboxylic group) compared with those in guanidinium benzenesulfonate G · BS. Generally, the one-dimensional arrangements in all three crystals comprise the same ribbon formations. However, the further organization of the ribbons is significantly different in G · CBS. We analyse the donor and acceptor efficacy of the additional functional group to disrupt some of the basic hydrogen bonds between the guanidinium and the sulfonium portions in G · BS. Since the carboxylic group introduces a mismatching of the sites on the counter ions, the changes in the symmetry relations essentially depend upon the topology of the substituent X, which results in modified packing patterns. All engineering peculiarities are analysed with respect to the symmetry constraints and geometrical demands of the packing forces.

Introduction

Crystal engineering is a vast and developing research area at the intersection of supramolecular, solid state and materials chemistry. At the present level of sophistication, it means the planning and execution of a crystal structure synthesis.[1] The crystal design methodology involves two main components; analysis of the ultimate constituents (molecules, ions) on the basis of their size, shape and intermolecular bonding capacity, and synthesis of hard supermolecules exploiting the connectivity based on supramolecular valence.[2] However, unlike organic molecular design, where almost any molecule can be synthesized with a high level of precision, the fidelity in crystal structure generation is still very limited. This is because our understanding of weak interactions is still unsatisfactory in the context of predictable organization and, especially, control of crystal nucleation.[3] The difficulties arise with the spatial complexity of intermolecular interactions and their weakness, so that even very subtle effects are decisive in determining the overall structure. In view of this, the need to divide the problem of three-dimensional assembly into less complicated sub-tasks is evident. The recognition of synthons as being inherently modular in their nature and imprinting the crystal structure broadened the horizons of crystal engineering.[4] The universality of those *n*-dimensional modules rests in the topological similarity of their constituents and allows for versatile structural design.[5] The multiplicity of hydrogen bonds employed in the modular units decides the stability of the two-dimensional networks that are less liable to additional effects of other weak interactions. Non-specific interactions introduced by ancillary groups, although decisive in the ultimate crystal packing, most often affect only to a limited extent the molecular assembly by deforming the basic hydrogen-bonded network. However, they are not capable of disrupting and totally reorganizing the primary network as long as dramatic impediments are not introduced. The advantage of the modular approach is demonstrated in the wide variety of two-dimensional hydrogen-bonded molecular networks reported during the last decade.[6] Metal-coordination and organometallic networks, hydrogen-bonded or constructed *via* other less directional interactions, have also been successfully designed.[7] Thus, the basic principles of inorganic crystal engineering have also started to be developed,[8] in addition to those of organic crystal engineering.[9]

The two-dimensional hydrogen-bonded sheets formed by guanidinium and sulfonate ions have been shown to be very flexible.[5a–c] The proton donor and acceptor sites in guanidinium benzenesulfonate are separate and explicitly located on the guanidinium cation and the sulfonate anion, respectively. Hence, the counter ions are matched in terms of symmetry and number of hydrogen-bonding atoms. The crystal chemical unit (CCU)[10] comprising the eight-membered ring motif R2,2(8)[11] is formed *via* two hydrogen bonds between two nitrogen atoms of a single guanidinium ion and two oxygen atoms of a single sulfonate group. They are further translationally or reflectionally extended into ribbons *via* two more hydrogen bonds, donated from the nitrogen atoms located on the same guanidinium ion toward the lone pairs of

---

† Electronic supplementary information (ESI) available: X-Ray powder diffraction spectra of **2** and **3** compared with those of their constituents. See http://www.rsc.org/suppdata/nj/b0/b009197i/

DOI: 10.1039/b009197i

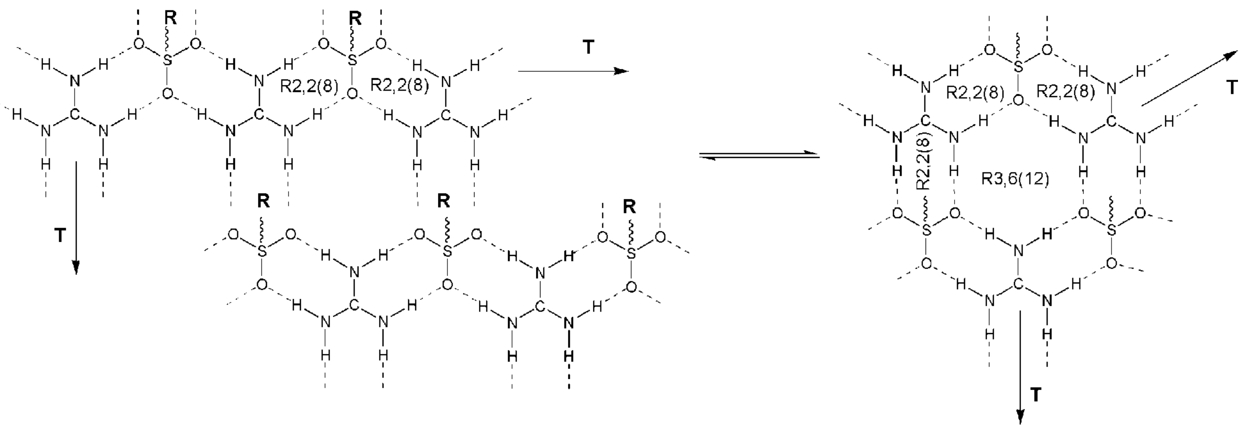

Scheme 1

two oxygen atoms belonging to the nearest sulfonate group with subsequent formation of a new R2,2(8) ring. The topology of the remaining two hydrogen-bond donors and two acceptors, so far not used, accommodates the parallel alignment of the ribbons into hydrogen-bonded sheets (Scheme 1). The planarity of the sheets essentially depends upon the interactions between the ancillary **R** groups and is defined by the dihedral angle θ_{IR} between the ribbons. In fact, the two-dimensional network can be considered as a two-dimensional propagation of the nano-sized R3,6(12) module, consisting of three pairs of R2,2(8) rings. However, the chemical nature and steric demands of the **R** group play a decisive role in the final crystal network organization, resulting in either mono- or bilayer (lamellar) structures.[5]

In the present work, we report on the structural proclivity in guanidinium carboxybenzenesulfonates $[C(NH_2)_3]^+[XC_6H_4SO_3]^-$ instigated by the topology of the additional functional group X (X = carboxylic group). We consider the concomitance of the sulfonic and carboxylic groups that are strongly competitive for hydrogen bond formation, and therefore, for crystal network organization. The structural studies of guanidinium 3-carboxybenzenesulfonate (G · 3CBS) **2** and guanidinium 4-carboxybenzenesulfonate (G · 4CBS) **3**, compared with those of guanidinium bensenesulfonate (G · BS)[5a] **1** (Scheme 2) are aimed at revealing the packing consequences and organizational peculiarities from an engineering point of view. The most important results of these studies are summarized in Table 1 and Fig. 1.

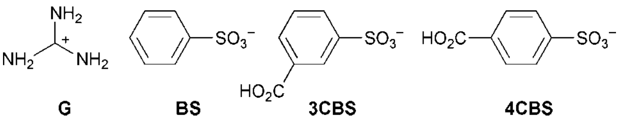

Scheme 2

Table 1 Unit cell parameters of the cocrystals **1**–**3**

Crystal lattice	G · BS (**1**)[5a]	G · 3CBS (**2**)	G · 4CBS (**3**)
Space group	$P2_1/c$	$P2_1/c$	$P2_1/c$
Z	8	8	4
a/Å	7.50(1)	7.701(1)	10.626(2)
b/Å	23.287(6)	30.779(6)	15.597(3)
c/Å	12.060(2)	9.425(2)	7.1820(10)
β/°	92.24(8)	92.98(3)	103.38(2)
V/Å^3	2104(4)	2231.0(9)	1158.0(4)
V/Z (Å^3 CCU^{-1})	263	279	289.5

Results and discussion

Crystal structure and hydrogen-bonded networks

Generally, the CCU formation and one-dimensional ribbon arrangement in **2** and **3** are the same as those in **1**. The first surmise for 3D organization in **2** and **3** was that the carboxylic groups should interconnect the opposite hydrogen-bonded sheets forming 'genuine' ring motifs[11] inside the bilayers. However, a careful analysis of the packing consequences resulted in this model being discarded. Should this scenario be correct, the unit cell parameter b should become twice as long as that in **1**, since the approximate interdistances between the hydrogen-bonded sheets are calculated to be 14.5 and 16.1 Å for **2** and **3**, respectively, *vs.* 7.11 Å in **1**. Obviously, this is not possible due to the demands of crystal packing. If the packing coefficients are to be within the reasonable limits of 0.65–0.77,[12] the permitted increase in the crystal unit cell, resulting from the additional volume increment of the carboxylic group (23.1 Å^3), is limited to only 11.4–13.5%.

The structural analysis reveals significant changes in the symmetry relations in **2** and **3**. The carboxylic group, exhibiting both donor and acceptor features, introduces mismatching of the hydrogen-bonding sites on the counter ions.

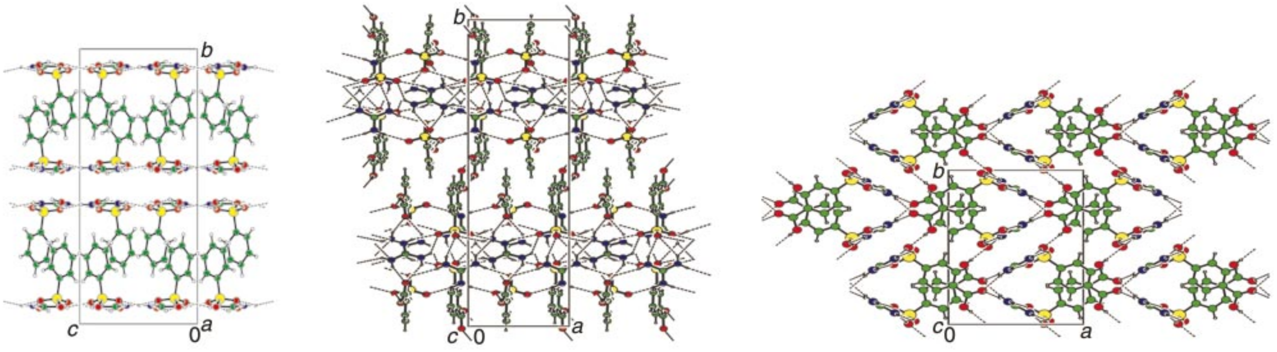

Fig. 1 The crystal packings viewed along the hydrogen-bonded layers in **1**–**3** show the bilayer structure in guanidinium benzenesulfonate (left) and the structural modifications in guanidinium 3-carboxybenzenesulfonate (centre) and guanidinium 4-carboxybenzenesulfonate (right). The separation of polar and non-polar regions alternates along the b-axis in **1** and **2**, and along the a-axis in **3**.

Table 2 Selected intramolecular bond lengths (Å) and angles (°) in **2** and **3**

Guanidinium 3-carboxybenzenesulfonate **2**					
Asymmetric unit A		Asymmetric unit B		Guanidinium 4-carboxybenxenesulfonate **3**	
S1A–O1A	1.445(2)	S1B–O1B	1.431(3)	S1–O1	1.4429(15)
S1A–O2A	1.452(2)	S1B–O2B	1.439(3)	S1–O2	1.4557(15)
S1A–O3A	1.460(2)	S1B–O3B	1.450(3)	S1–O3	1.4632(14)
S1A–C1A	1.771(3)	S1B–C1B	1.770(3)	S1–C1	1.775(3)
C7A–C3A	1.485(4)	C7B–C3B	1.478(4)	C7–C4	1.487(3)
C7A–O4A	1.204(4)	C7B–O4B	1.234(4)	C7–O4	1.211(3)
C7A–O5A	1.321(4)	C7B–O5B	1.299(4)	C7–O5	1.307(2)
O5–H1(O5)	0.79(5)	O5–H2(O5)	0.78(6)	O5–H(O5)	0.73(4)
C8A–N1A	1.313(4)	C8B–N1B	1.304(4)	C8–N1	1.316(3)
C8A–N2A	1.320(4)	C8B–N2B	1.313(4)	C8–N2	1.316(3)
C8A–N3A	1.321(4)	C8B–N3B	1.323(4)	C8–N3	1.318(3)
O1A–S1A–O2A	113.79(14)	O1B–S1B–O2B	111.62(16)	O1–S1–O2	113.76(9)
O1A–S1A–O3A	111.35(13)	O1B–S1B–O3B	112.94(15)	O1–S1–O3	112.85(8)
O2A–S1A–O3A	112.09(14)	O2B–S1B–O3B	112.16(15)	O2–S1–O3	110.88(9)
C1A–S1A–O1A	106.60(14)	C1B–S1B–O1B	106.69(15)	C1–S1–O1	106.42(9)
C1A–S1A–O2A	106.77(13)	C1B–S1B–O2B	106.15(15)	C1–S1–O2	106.68(9)
C1A–S1A–O3A	105.64(14)	C1B–S1B–O3B	106.76(14)	C1–S1–O3	105.61(8)
C3A–C7A–O4A	123.1(3)	C3B–C7B–O4B	121.7(3)	C4–C7–O4	123.69(18)
C3A–C7A–O5A	112.5(3)	C3B–C7B–O5B	115.3(3)	C4–C7–O5	113.31(19)
O4A–C7A–O5A	124.5(3)	O4B–C7B–O5B	123.1(3)	O4–C7–O5	123.0(2)
N1A–C8A–N2A	120.6(3)	N1B–C8B–N2B	120.7(3)	N1–C8–N2	120.5(2)
N1A–C8A–N3A	120.2(3)	N1B–C8B–N3B	119.8(3)	N1–C8–N3	119.5(2)
N2A–C8A–N3A	119.2(3)	N2B–C8B–N3B	119.4(3)	N2–C8–N3	120.0(2)

Table 3 Hydrogen bond geometries of **2** and **3**

Hydrogen bond interactions	R(H···B)/Å	R(A···B)/Å	θ(A–H···B)/°	Symmetry code	H.B. motif
Co-crystal **2**	A-network				
	A-CCU formation				
N1A–H21A···O1A	2.04(4)	2.891(4)	170(4)	x, y, z	R2,2(8)
N2A–H22A···O2A	2.18(4)	2.969(4)	166(3)	x, y, z	
	A-ribbon formation			Translation along x	
N1A–H11A···O3A	2.13(5)	2.935(4)	172(4)	$x + 1, y, z$	R2,2(8)
N3A–H13A···O2A	2.19(4)	2.990(4)	171(4)	$x + 1, y, z$	
	Pleated sheet formation			Translation along z	
O5A–H1(O5A)···O3A	1.90(5)	2.684(4)	170(5)	$x, y, z + 1$	C(8)
	B-network				
	B-CCU formation			b-glide	
N1B–H11B···O2B	2.11(4)	2.828(4)	156(4)	$x, \bar{y} + 1/2, z + 3/2$	R1,2(6)
N2B–H12B···O2B	2.29(4)	3.005(5)	140(3)	$x, \bar{y} + 1/2, z + 3/2$	
	B-chain formation			Translation along x	
N1B–H21B···O1B	1.91(5)	2.841(4)	174(3)	$x - 1, \bar{y} + 1/2, z + 3/2$	D
	B-chain–B-chain dimerization			Inversion and translation along x	
O5B–H2(O5B)···O4B	1.90(6)	2.662(4)	167(6)	$\bar{x} - 2, \bar{y}, \bar{z}$	R2,2(8)
	B-chain–B-chain association			Translation along z	
N3B–H13B···O3B	2.57(5)	2.976(4)	111(4)	$x - 1, y, z + 1$	D
A–B network interactions	A-ribbon–B-chain linking			b-glide	
N3B–H23B···O4A	2.20(4)	2.937(4)	159(4)	x, y, z	R1,2(6)
N2B–H22B···O4A	2.47(5)	3.188(5)	146(4)	x, y, z	
N3A–H23A···O3B	2.58(5)	3.296(4)	145(4)	$x, \bar{y} + 1/2, z + 1/2$	R1,2(6)
N2A–H12A···O3B	2.28(5)	3.034(4)	160(4)	$x, \bar{y} + 1/2, z + 1/2$	
				b-glide and translation along x and z	
N3A–H23A···N3B(sp^3)	2.60(5)	3.291(5)	142(4)	$x + 1, \bar{y} + 1/2, z - 1/2$	
Co-crystal **3**					
	CCU formation				
N2–H2(N2)···O2	2.05(3)	2.901(3)	171(3)	x, y, z	R2,2(8)
N1–H1(N1)···O1	0.23(3)	2.935(3)	167(3)	x, y, z	
	Ribbon formation			Translation along z	
N1–H2(N1)···O3	2.07(3)	2.897(3)	177(2)	$x, y, z + 1$	R2,2(8)
N3–H2(N3)···O2	2.14(3)	2.967(3)	169(2)	$x, y, z + 1$	
	Ribbon association			$2_1(y)$ screw rotation and translation along z	
O5–H1(O5A)···O3	1.91(4)	2.632(2)	176(4)	$\bar{x}, y + 1/2, \bar{z} - 1/2$	C(9)
	Ribbon association			Translation along x	
N2–H1(N2)···O4	2.15(3)	2.956(3)	162(3)	$x + 1, y, z + 1$	D
	Ribbon association			b-glide and translation along y	
N3–H1(N3)···O4	2.56(3)	3.077(3)	124(2)	$x + 1, \bar{y} + 3/2, z + 3/2$	D

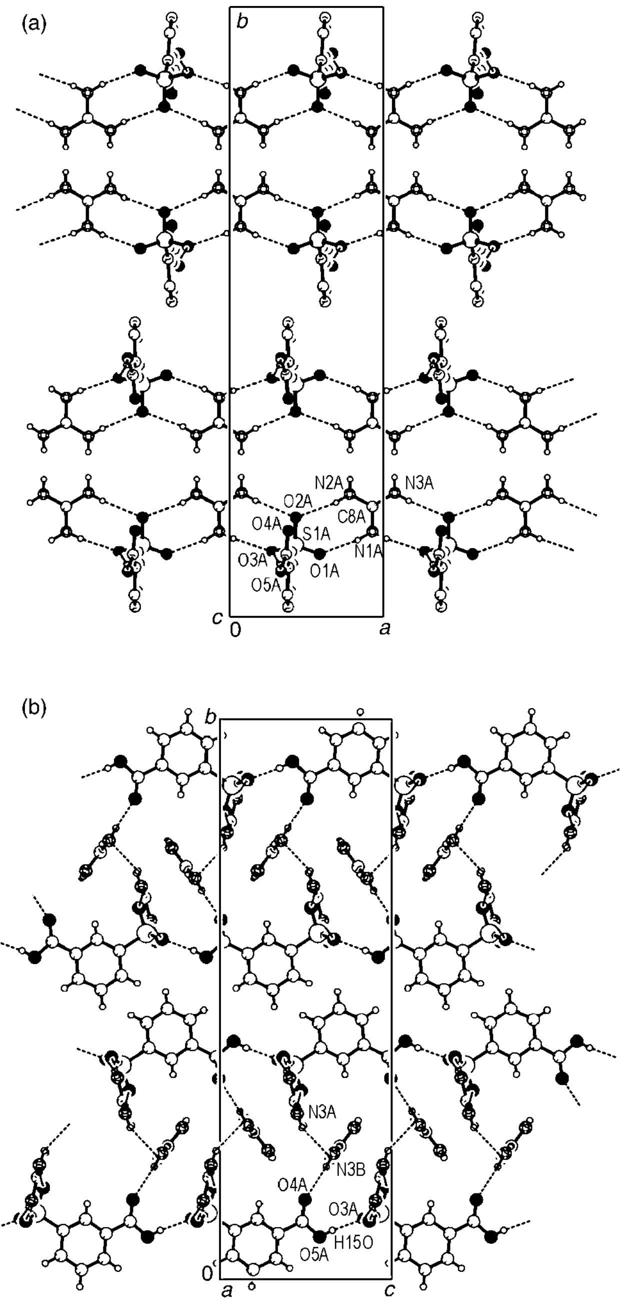

Fig. 2 Two different presentations of the A-subnetwork in guanidinium 3-carboxybenzenesulfonate: (a) the view along the *c*-axis shows the hydrogen-bonded ribbons and reveals the inter-ribbon symmetry and distance relations of the polar and non-polar regions: the carboxylic groups are protruding out of the plane of the page. (b) The view along the hydrogen-bonded ribbons shows their collation to form pleated sheets and reveals the symmetry and distance relations of the arene rings gallery. The unusual hydrogen bonding [N3A–H2(N3A)···N3B] between the A and B guanidinium ions is also shown.

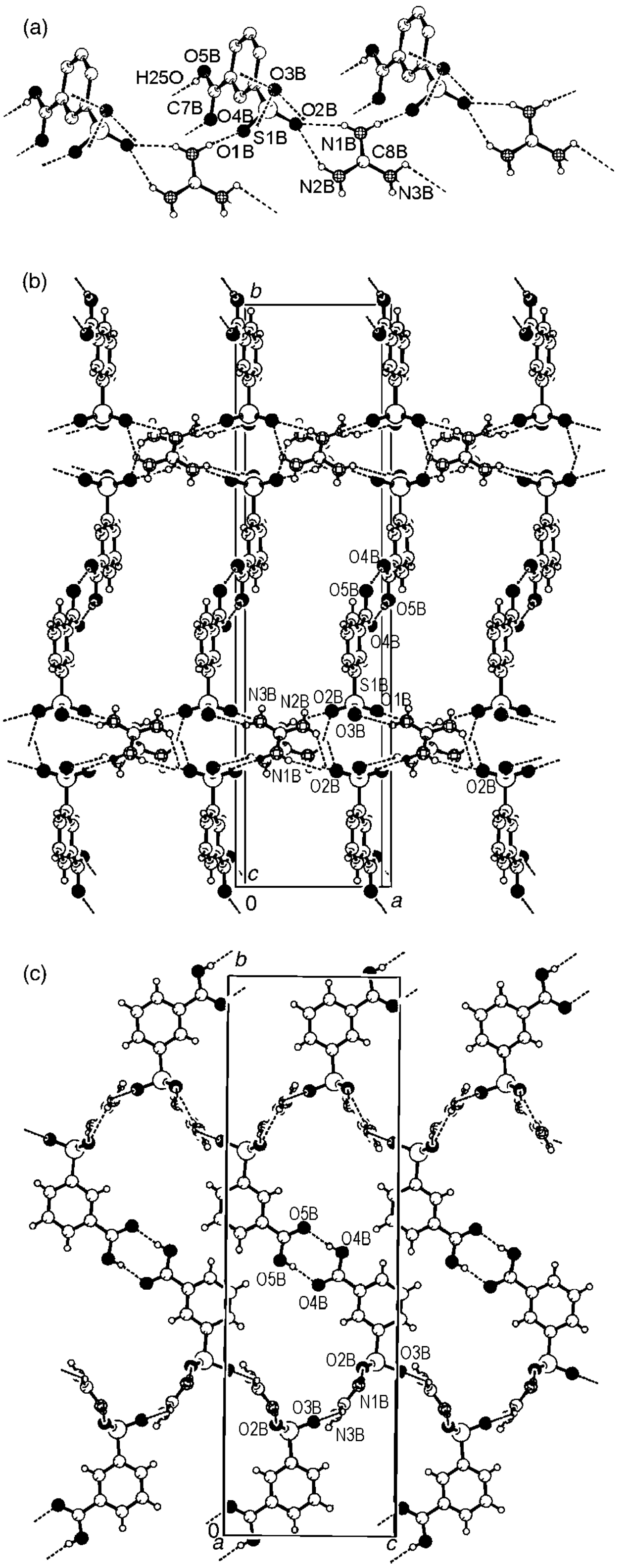

Fig. 3 Three different views of the B-subnetwork in guanidinium 3-carboxybenzenesulfonate: (a) view of the intra-chain hydrogen bond relations; (b) view along the *c*-axis showing the inter-chain relations in the outer polar region; (c) view along the *a*-axis showing the benzene ring arrangement and the inter-chain relations in the inner non-polar region. The interplay of A and B-subnetworks furnishing the overall crystal structure is shown in Fig. 1(b).

The carboxylic hydrogen, as a better donor[13] than the guanidinium hydrogens, and the carbonyl oxygen, as a better acceptor than the sulfonate oxygens, enforce a quite different linking mechanism in the second and third dimensions (Tables 2 and 3).

Two independent asymmetric units, denoted as CCU-A and CCU-B, generate the crystal network in **2**. The A-units are arranged into *a*-translationally related one-dimensional ribbons *via* four hydrogen bonds donated from the guanidinium cation toward the sulfonate portion of the anions: two of them [N1A–H2(N1A)···O1A and N2–H2(N2A)···O2A] form the CCU whereas the other two [N1A–H1(N1A)···O3A and N3A–H1(N3A)···O2A] link the units [Fig. 2(a)]. However, the inter-ribbon relations in **2** are significantly different from those in **1**.[5a] The *meta*-position of the carboxylic group *vs.* the sulfonic group reinforces the hydrogen bond competition for a two-dimensional arrangement. The remaining two guanidinium–sulfonate hydrogen

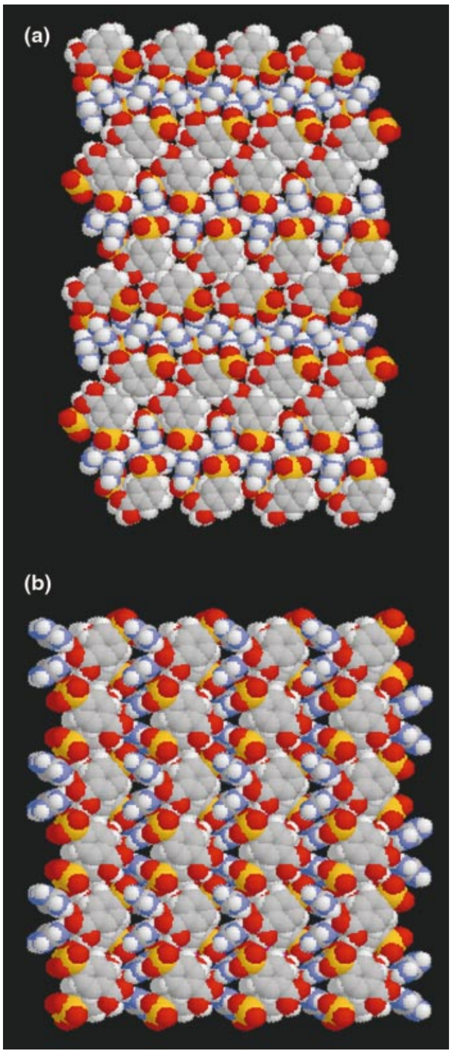

Fig. 4 Space-filling representation of the three-dimensional crystal packing in guanidinium 3-carboxybenzenesulfonate (a) and guanidinium 4-carboxybenzenesulfonate (b).

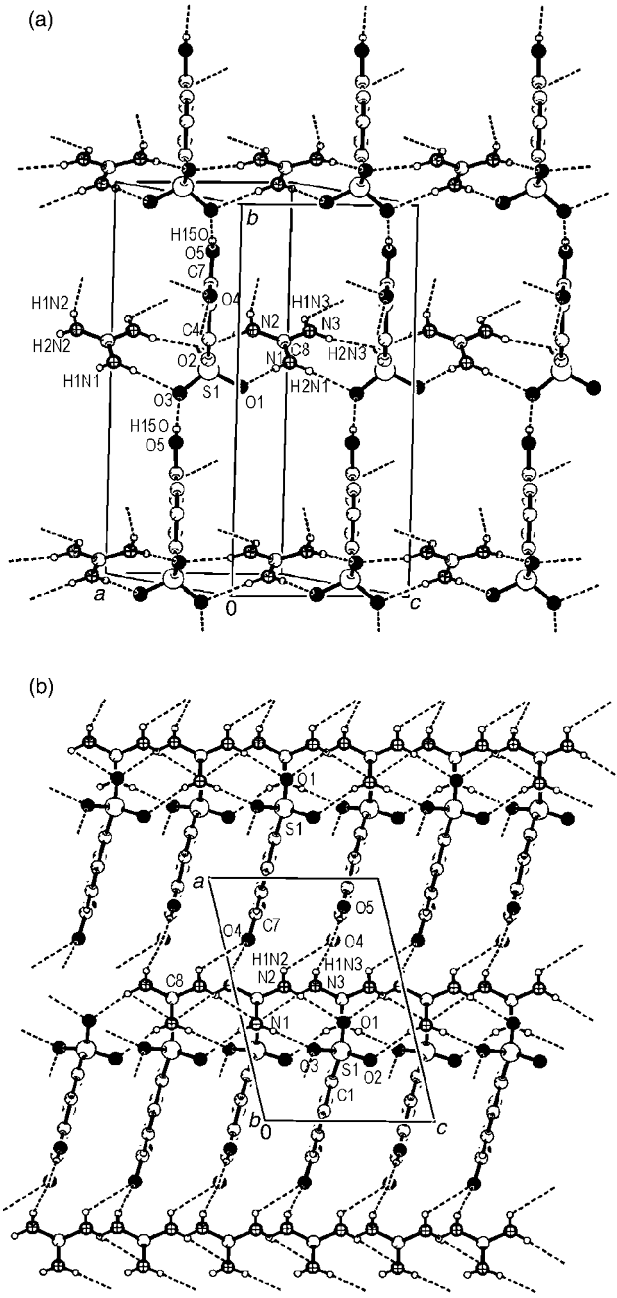

Fig. 5 A view of the glide-related hydrogen-bonded ribbons in **3**, conjoined *via* strong O5–H1(O5)···O3 hydrogen-bonds (a); two more hydrogen bonds donated from the remaining two guanidinium hydrogens toward a single carboxylic oxygen (O4) complete the three-dimensional network (b). The hydrogen atoms of the benzene rings are omitted.

bonds, N1···O1 and N3···O3, that conjoin the ribbons in **1** become disregarded in **2**, where the single, very strong hydrogen bond O5A–H1(O5A)···O3A between the carboxylic and the sulfonate portions is used to fasten the ribbons in the second dimension [Fig. 2(b)]. As a result, the A-ribbons tilt significantly toward the (001) plane and collate along the *c*-direction in order to accommodate the geometrical and sterical constraints for close packing. The almost planar hydrogen-bonded sheets ($\theta_{IR} = 150°$) in **1** transform into pleated sheets ($\theta_{IR} = 7°$) in **2** which is followed by a shrinkage of the unit cell parameter *c* (see Table 1). The A-benzene rings become locked between the ribbons and aligned parallel to the (100) plane. Thus, the van der Waals (vdW) interactions governing the arene gallery change from edge-to-face (EF) in **1** to offset face-to-face (OFF) in **2**. The mean distance between the planes of opposite aryl rings becomes 3.029 Å. The two parameters d_{np} and d_p, characterizing the thickness of the hydrophobic (non-polar) and the hydrophilic (polar) regions, change significantly. The mean distance d_{np} between the inversion-related pleated sheets reduces to 5.971 Å, compared to 8.31 Å for the intralamellar distance in **1**. On the other side, the parameter d_p (3.33 Å in **1**) expands to 9.419 Å which is far beyond the range of any packing forces if the B-subunits were not present. The B-sublattice is organized in a manner able to adapt the steric and directional constraints dictated by the rigid A-network. A pliant **R**1,2(6) ring motif incorporating two hydrogen bonds donated from two nitrogens (N1B and N2B) toward a single sulfonate oxygen (O2B) is used for the formation of the B-CCUs, which are further flexibly extended into chains [*via* the single hydrogen bond N1B–H2(N1B)···O1B] running in the same direction as the A-ribbons [Fig. 3(a)]. The rigid dimer association *via* O5B–H2(O5B)···O4B between the carboxylic groups inside the arene region moves the inversion-related chains far apart, placing them in the outside polar region between the A-sheets [Fig. 3(c)]. The loose arrangement of translationally related B-chains [*via* N3B–H1(N3B)···O3B] in the outside region relieves the tension of the inside region [Fig. 3(b)]. Four more N–H···O-type hydrogen bonds complete the final crystal network. Two of them are directed from A-guanidinium to B-sulfonate and two more from B-guanidinium to A-sulfonate residues. They are all collocated in the outside region between the pleated sheets and join the ribbons with the chains in the third dimension, using two more **R**1,2(6) ring motifs. The overall crystal lattice [Fig. 4(a)] demonstrates an apparent separation of different interaction regions alternating along the monoclinic *b*-axis, which makes the meaning of d_{np} and d_p clear. The non-polar regions contain the arene rings and are ruled by the inversion symmetry operator, whereas the glide reflection operator governs the interactions in the polar regions, comprising the hydrogen-bonded A-ribbons and B-chains. The extraordinary hydrogen bonding [N3A–H2(N3A)···N3B] between the A and B guanidinium ions [see Table 3 and Fig. 2(b)] deserves some comment because it is donated from the H2(N3A) atom, which is already used in the formation of another hydrogen bond and, thus, serves as a bifurcated donor. Even more peculiar is the fact that it is donated toward the lone pair of the guanidinium nitrogen atom N3B, with a resultant change in the electronic configuration from trigonal pyramidal to tetragonal, which is a quite rare phenomenon.

Substitution of the carboxylic group in the *para*-position makes it even more competitive for 3D network organization and results in a reduction of the crystal unit cell and a reorientation of the polar and non-polar regions alternating along the crystallographic *a*-axis. The one-dimensional arrangement in **3** is the same as in the former crystals, although the ribbons run along the *c*-axis [Fig. 5(a)]. However, the two-dimensional hydrogen-bonded sheet and the bilayer structure become strongly disrupted by the presence of the very efficient donor and acceptor sites positioned exactly opposite to the sulfonic group. The sulfonate–guanidinium interactions between the glide-related CCUs are discarded in favour of the single very strong hydrogen bond O5–H1(O5)···O3 conjoining the screw-related ribbons and scaffolding the anions into zig-zag chains along the *b*-axis. On the other side, the lone pairs on the carbonyl oxygen O4 are sterically and geometrically accessible for two discarded proton donors located on different guanidinium portions. Head-to-tail arrangement of the translationally related ribbons [*via* N2–H1(N2)···O4] and the glide-reflected ribbons [*via* N3–H1(N3)···O4] [Fig. 5(b)], affiliates the formal monolayers into hydrogen-bonded interwoven layers (as opposed to the bilayer structure in **1**). Thus, the carboxylic group in **3** acts as a specific three-dimensional conjunction for the ribbons. For the obvious reasons of hydrogen bond geometry demands, the planes of the hydrogen-bonded ribbons tilt out of the (010) plane forming a dihedral angle of $\pm 55°$ with the (100) plane. Therefore, the crystal structure of **3** is better described with two separate interaction regions alternating along the crystal *a*-axis [Fig. 4(b)]. The non-isotropic (polar) regions at 1/2*a*, 3/2*a*, 5/2*a*, . . . are dominated by directional interactions between the subunits. The isotropic (vdW) regions arranged at 0, 1*a*, 2*a*, . . . are covered by face-to-face (FF) interactions between the aromatic rings (see Fig. 1).

Conclusions

In this study, we have elucidated the organizational competition between the sulfonic and carboxylic groups and revealed the packing consequences resulting from their topologies. In agreement with our initial predictions, the additional hydrogen bond capacity introduced by the carboxylic group causes significant structural modifications in **2** and **3** compared to **1**.

Whereas the complete separation of the donor and acceptor sites in **1** generates a separation of the isotropic and non-isotropic interaction regions with formation of a resultant bilayer (lamellar) structure in **1**, the mismatching of those sites in **2** and **3** forces a prominent reorganization of their crystal networks. The ionic interactions between the bilayers in **1** are replaced by hydrogen bonds between the carboxylic group and the guanidinium ion that modify the interlamellar space and generate thick monolayers (polar regions) in **2** and **3**. As already discussed, the symmetry relations dictated by the directional forces in these carboxy–guanidinium–sulfonate monolayers are much more complicated than those in the guanidinium–sulfonate sheets in **1**. Under these circumstances, new packing forces are required to allow the aromatic portions in **2** and **3** to adapt to the requirements of the basic hydrogen-bonded networks. The edge-to-face (EF) interactions governing the benzene ring galleries (at 1/4*b*, 3/4*b*, 5/4*b*, . . .) in **1** convert to offset face-to-face (OFF) interactions and to face-to-face (FF) interactions, which control the corresponding regions in **2** and **3**. As a consequence, the non-polar regions, created by the aromatic parts, alternate along the *b*-axis at 0*b*, 1/2*b*, 3/2*b*, 5/2*b*, . . . in **2** and along the *a*-axis at 0*a*, 1*a*, 2*a*, . . . in **3** (see Table 1).

Experimental

General procedures

All commercially available starting materials were purchased from Aldrich and used without further purification. Spectroscopic grade solvents and/or deionised water were used for all crystallizations. Melting points were determined with a Bethius plate and are uncorrected. Solid-state infrared spectra were recorded on a Perkin-Elmer 1600 FTIR spectrometer (4 cm^{-1} resolution) from Nujol mulls and KBr pellets and compared with those of the starting materials. Powder diffraction measurements were performed on a Philips X'Pert instrument (40 kV, 30 mA, Cu-Kα_1 radiation).

Syntheses

Guanidinium 3-carboxybenzenesulfonate, 2. Compound **2** was crystallized from an aqueous solution containing equimolar quantities of guanidine hydrochloride and sodium 3-carboxybenzenesulfonate using slow evaporation techniques. After seven weeks, colourless plates were obtained. The product homogeneity was tested by comparing the powder diffraction spectra of the product and the starting materials (see ESI) and melting point measurements (m.p. 210–212 °C), and characterized by IR spectroscopy: ν/cm^{-1} 3481, 3448, 3369, 3200, 2889, 2660, 2545, 2360, 1714, 1655, 1600, 1575, 1475, 1430, 1420, 1308, 1293, 1278, 1220, 1194, 1142, 1095, 1076, 1040, 1033, 996, 930, 915, 904, 846, 810, 753, 730, 680, 655, 617, 572, 535, 490.

Guanidinium 4-carboxybenzenesulfonate, 3. Compound **3** was crystallized from an aqueous solution containing equimolar quantities of guanidine hydrochloride and potassium 4-carboxybenzenesulfonate using slow evaporation techniques. After three weeks, colourless needles were obtained and recrystallised in order to obtain single crystals of better quality. The product homogeneity was tested by powder diffraction spectroscopy (see ESI) and melting point measurements (m.p. 278–280 °C), and characterized by IR spectroscopy: ν/cm^{-1} 3477, 3428, 3362, 3260, 3200, 2890, 2639, 2496, 1685, 1647, 1575, 1495, 1419, 1306, 1252, 1232, 1185, 1165, 1130, 1110, 1030, 1005, 977, 911, 859, 809, 769, 711, 685, 642, 630, 579, 560, 535.

X-Ray crystallography

Data collection on a KM4CCD diffractometer with graphite-monochromated Mo-Kα radiation ($\lambda = 0.71073$ Å) at 293 K. Programs used for structure solutions: SHELX-93 (for **2**) and SHELX-97 (for **3**).[14] Hydrogen atoms were located from the difference map and a riding model with fixed thermal parameters [$U_{ij} = 1.2U_{ij}$(eq)] for the atom to which they are bonded was used for subsequent refinements. Corrections made: secondary extinction coefficient 0.0152(33) for **2** and 0.0172(16) for **3**. The computer program PLATON[15] was used to analyze the geometry of the hydrogen-bonding patterns. RasMol[16] and PLATON were used for graphical representation of the results.

Crystal data for 2. $C_8H_{11}N_3O_5S$, $M_r = 261.27$ g mol^{-1}, colourless plate ($0.6 \times 0.4 \times 0.2$ mm), monoclinic, space group $P2_1/c$ (no. 14), $1.3 \leqslant \theta \leqslant 25.0°$; $a = 7.701(2)$, $b = 30.779(6)$, $c = 9.425(2)$ Å, $\beta = 92.98(3)°$, $Z = 8$, $V = 2231.0(9)$ Å^3, $D_c = 1.556$ Mg m^{-3}, $F(000) = 1088$, $\mu = 0.306$ mm^{-1}, 10 958 reflections measured, 3914 independent, 3510 considered observed $[I > 2\sigma(I)]$; 396 parameters, $R_{all} = 0.0593$, $R_{obs} = 0.0512$, $wR_{all} = 0.1446$, $wR_{obs} = 0.1346$, $S = 1.21$, $\rho_{min/max} = -0.29$, 0.42 e Å^{-3}.

Crystal data for 3. $C_8H_{11}N_3O_5S$, $M_r = 261.27$ g mol^{-1}, colourless needle, monoclinic, space group $P2_1/c$ (no. 14), $3.9 \leqslant \theta \leqslant 26.0°$; $a = 10.626(2)$, $b = 15.597(3)$, $c = 7.1820(10)$ Å, $\beta = 103.38(2)°$, $Z = 4$, $V = 1158.0(4)$ Å^3, $D_c = 1.499$ Mg m^{-3}, $F(000) = 544$, $\mu = 0.294$ mm^{-1}, 6766 reflections measured, 2264 independent, 2152 considered observed $[I > 2\sigma(I)]$; 199 parameters, $R_{all} = 0.0445$, $R_{obs} = 0.0428$, $wR_{all} = 0.1203$, $wR_{obs} = 0.1180$, $S = 1.12$, $\rho_{min/max} = -0.40$, 0.28 e Å^{-3}.

CCDC reference numbers 145854 and 145855. See http://www.rsc.org/suppdata/b0/b009197i/ for crystallographic data in CIF or other electronic format.

Acknowledgements

Financial support by The Centre of Nanotechnology and Advanced Materials (project "Noncovalent synthesis. Topochemical control of supramolecular synthesis") and by the Wrocław University of Technology (project "Intermolecular interactions in a supramolecular aspect") is gratefully acknowledged.

References and notes

1 G. R. Desiraju, *Chem. Commun.*, 1997, 1475.

2 D. Braga, F. Grepioni and G. R. Desiraju, *Chem. Rev.*, 1998, **98**, 1375.

3 A. Gavezzotti, *Acc. Chem. Res.*, 1994, **27**, 309.

4 (*a*) G. R. Desiraju, *Angew. Chem., Int. Ed. Engl.*, 1995, **34**, 2311; (*b*) D. S. Reddy, D. C. Craig and G. R. Desiraju, *J. Am. Chem. Soc.*, 1996, **118**, 4090; (*c*) D. S. Reddy, Yu. E. Ovchinnikov, O. V. Shishkin, Yu. T. Struchkov and G. R. Desiraju, *J. Am. Chem. Soc.*, 1996, **118**, 4085; (*d*) J. A. R. P. Sarma, F. H. Allen, V. J. Hoy, J. A. K. Howard, R. Thaimattam, K. Biradha and G. R. Desiraju, *Chem. Commun.*, 1997, 101; (*e*) J. Starbuck, N. C. Norman and A. G. Orpen, *New J. Chem.*, 1999, **23**, 969.

5 (*a*) V. A. Russell, M. C. Etter and M. D. Ward, *J. Am. Chem. Soc.*, 1994, **116**, 1941; (*b*) V. A. Russell, M. C. Etter and M. D. Ward, *Chem. Mater.*, 1994, **6**, 1206; (*c*) V. A. Russell and M. D. Ward, *Chem. Mater.*, 1996, **8**, 1654; (*d*) V. A. Russell and M. D. Ward, *Acta Crystallogr., Sect. B*, 1996, **52**, 209; (*e*) V. A. Russell and M. D. Ward, *J. Mater. Chem.*, 1997, **7**, 1123; (*f*) V. A. Russell, C. C. Evans, W. Li and M. D. Ward, *Science*, 1997, **276**, 575; (*g*) C. C. Evans, L. Sukarto and M. D. Ward, *J. Am. Chem. Soc.*, 1999, **121**, 320.

6 (*a*) J.-M. Lehn, M. Mascal, A. DeCian and J. Fischer, *J. Chem. Soc., Chem. Commun.*, 1990, 479; (*b*) J. A. Zerkowski, J. A. MacDonald, C. T. Seto, D. A. Wierda and G. Whitesides, *J. Am. Chem. Soc.*, 1994, **116**, 2382; (*c*) J. A. Zerkowski, J. A. MacDonald and G. M. Whitesides, *Chem. Mater.*, 1994, **6**, 1250; (*d*) C. V. K. Sharma, C. B. Bauer, R. D. Roger and M. J. Zaworotko, *Chem. Commun.*, 1997, 1559; (*e*) K. Biradha, D. Dennis, V. A. MacKinnon, C. V. K. Sharma and M. J. Zaworotko, *J. Am. Chem. Soc.*, 1998, **120**, 11894; (*f*) C. B. Aakeröy and P. B. Hitchcock, *J. Mater. Chem.*, 1993, **3**, 1129; (*g*) C. B. Aakeröy and M. Nieuwenhuyzen, *J. Am. Chem. Soc.*, 1994, **116**, 10983; (*h*) V. Videnova-Adrabińska, *J. Mol. Struct.*, 1996, **374**, 199; (*i*) V. Videnova-Adrabińska and E. Janeczko, *J. Mater. Chem.*, 2000, **10**, 555; (*j*) F. Xue and T. C. W. Mak, *Acta Crystallogr., Sect. B*, 2000, **56**, 142; (*k*) T. C. W. Mak and F. Xue, *J. Am. Chem. Soc.*, 2000, **122**, 9860.

7 (*a*) A. Müller, H. Reuter and S. Dillinger, *Angew. Chem., Int. Ed. Engl.*, 1995, **34**, 2328; (*b*) D. Braga, C. Bazzi, L. Maini and F. Grepioni, *CrystEngComm.*, 1999, **5**; D. Braga, F. Grepioni and G. R. Desiraju, *Chem. Rev.*, 1998, **98**, 1375; (*d*) F. Grepioni, S. Gladiali, L. Scaccianoce, P. Ribeiro and D. Braga, *New J. Chem.*, 2001, **25**, 690; (*e*) A. D. Burros, C-W. Chen, M. M. Chowdry, J. E. McGrady and D. M. P. Mingos, *Chem. Soc. Rev.*, 1995, 329; (*f*) S. B. Copp, K. T. Holman, J. O. S. Sangster, S. Subramanian and M. J. Zaworotko, *J. Chem. Soc., Dalton Trans.*, 1995, 2233; (*g*) S. A. Bourne, J. Lu, B. Moulton and M. Zaworotko, *Chem. Commun.*, 2001, 861; (*h*) B. Moulton, J. Lu, A. Mondal and M. Zaworotko, *Chem. Commun.*, 2001, 263; (*i*) C. B. Aakeröy, A. M. Beatty and D. S. Leinen, *Angew. Chem., Int. Ed.*, 1999, **38**, 1815.

8 (*a*) D. Braga, *J. Chem. Soc., Dalton Trans.*, 2000, 3705; (*b*) G. R. Desiraju, *J. Chem. Soc., Dalton Trans.*, 2000, 3745.

9 (*a*) G. R. Desiraju, in *Comprehensive Supramolecular Chemistry*, ed. D. D. MacNicol, F. Toda and R. Bishop, Pergamon, Oxford, 1996 vol. 6; (*b*) *Perspectives in Supramolecular Chemistry: The Crystal as a Supramolecular Entity*, ed. G. R. Desiraju, Wiley, Chichester, 1996, vol. 2.

10 The crystal chemical unit (CCU) contains the complete unique molecules and ions that comprise the crystal structure and is synonymous with the asymmetric unit. For more details, see: F. H. Allen, O. Kennard, W. D. S. Motherwell, W. G. Town, T. J. Scott and A. C. Larson, *J. Appl. Crystallogr.*, 1974, **7**, 73. The CCUs in hydrogen-bonded ionic structures **1**–**3** can also be considered as bimolecular couplings (see: F. H. Allen, P. R. Raithby, G. S. Schields and R. Taylor, *Chem. Commun.*, 1998, 1043) or as comolecules [ref. (6*h*, *i*)].

11 For the graph set notation $X^a_d(n)$, see: (*a*) M. C. Etter, J. MacDonald and J. Bernstein, *Acta Crystallogr., Sect. B*, 1990, **46**, 256; (*b*) J. Bernstein, R. E. Davis, L. Shimoni and N.-L. Chang, *Angew. Chem., Int. Ed. Engl.*, 1995, **34**, 1555; J. Bernstein, R. E. Davis, L. Shimoni and N.-L. Chang, *Angew. Chem.*, 1995, **107**, 1689; (*c*) J. Grell, J. Bernstein and G. Tinhofer, *Acta Crystallogr., Sect. B*, 1999, **55**, 1030; For convenience, the alternative notation $Xa,d(n)$ is used in this paper (see: W. D. S. Motherwell, G. P. Shields and F. H. Allen, *Acta Crystallogr., Sect. B*, 1999, **55**, 1044). According to the definition for a "genuine" R2,2(8) intermolecular ring, only non-translational operations (inversion center, *n*-fold rotation or inversion axis, mirror plane) between the molecular units are allowed. Consistent with the assignment used for **1** in ref. 5(*a*) we also use this descriptor for ring motifs related by a translational element of symmetry. Thus, the PLUTO automatic procedure for computation of the graph set descriptors will not design all the ring motifs described in this paper.

12 A. I. Kitajgorodsky, *Molecular Crystals and Molecules*, Academic Press, New York/London, 1973.

13 For hydrogen bond rules, see: M. C. Etter, *Acc. Chem. Res.*, 1990, **23**, 120.

14 (*a*) G. M. Sheldrick, SHELX-93, Program for Refinement of Crystal Structures, University of Göttingen, Germany, 1993; (*b*) G. M. Sheldrick, SHELXS-97, Program for Refinement of Crystal Structures, University Göttingen, Germany, 1997.

15 A. L. Speck, PLATON, A Multipurpose Crystallographic Tool, Utrecht University, The Netherlands, 1999.

16 R. Sayle, RasMol v2.6, Molecular Visualisation Program, Glaxo Wellcome Research and Development, Stevenage, UK, 1995.